

Measurement of the forward-backward asymmetries in the production of Ξ and Ω baryons in $p\bar{p}$ collisions

V. M. Abazov,³¹ B. Abbott,⁶⁷ B. S. Acharya,²⁵ M. Adams,⁴⁶ T. Adams,⁴⁴ J. P. Agnew,⁴¹ G. D. Alexeev,³¹ G. Alkhazov,³⁵ A. Alton,^{56,a} A. Askew,⁴⁴ S. Atkins,⁵⁴ K. Augsten,⁷ V. Aushev,³⁸ Y. Aushev,³⁸ C. Avila,⁵ F. Badaud,¹⁰ L. Bagby,⁴⁵ B. Baldin,⁴⁵ D. V. Bandurin,⁷⁴ S. Banerjee,²⁵ E. Barberis,⁵⁵ P. Baringer,⁵³ J. F. Bartlett,⁴⁵ U. Bassler,³⁹ V. Bazterra,⁴⁶ A. Bean,⁵³ M. Begalli,² L. Bellantoni,⁴⁵ S. B. Beri,²³ G. Bernardi,¹⁴ R. Bernhard,¹⁹ I. Bertram,³⁹ M. Besançon,¹⁵ R. Beuselinck,⁴⁰ P. C. Bhat,⁴⁵ S. Bhatia,⁵⁸ V. Bhatnagar,²³ G. Blazey,⁴⁷ S. Blessing,⁴⁴ K. Bloom,⁵⁹ A. Boehnlein,⁴⁵ D. Boline,⁶⁴ E. E. Boos,³³ G. Borisso,³⁹ M. Borysova,^{38,l} A. Brandt,⁷¹ O. Brandt,²⁰ M. Brochmann,⁷⁵ R. Brock,⁵⁷ A. Bross,⁴⁵ D. Brown,¹⁴ X. B. Bu,⁴⁵ M. Buehler,⁴⁵ V. Buescher,²¹ V. Bunichev,³³ S. Burdin,^{39,c} C. P. Buszello,³⁷ E. Camacho-Pérez,²⁸ B. C. K. Casey,⁴⁵ H. Castilla-Valdez,²⁸ S. Caughron,⁵⁷ S. Chakrabarti,⁶⁴ K. M. Chan,⁵¹ A. Chandra,⁷³ E. Chapon,¹⁵ G. Chen,⁵³ S. W. Cho,²⁷ S. Choi,²⁷ B. Choudhary,²⁴ S. Cihangir,^{45,*} D. Claes,⁵⁹ J. Clutter,⁵³ M. Cooke,^{45,l} W. E. Cooper,⁴⁵ M. Corcoran,⁷³ F. Couderc,¹⁵ M. -C. Cousinou,¹² J. Cuth,²¹ D. Cutts,⁷⁰ A. Das,⁷² G. Davies,⁴⁰ S. J. de Jong,^{29,30} E. De La Cruz-Burelo,²⁸ F. Déliot,¹⁵ R. Demina,⁶³ D. Denisov,⁴⁵ S. P. Denisov,³⁴ S. Desai,⁴⁵ C. Deterre,^{41,d} K. DeVaughan,⁵⁹ H. T. Diehl,⁴⁵ M. Diesburg,⁴⁵ P. F. Ding,⁴¹ A. Dominguez,⁵⁹ A. Dubey,²⁴ L. V. Dudko,³³ A. Duperrin,¹² S. Dutt,²³ M. Eads,⁴⁷ D. Edmunds,⁵⁷ J. Ellison,⁴³ V. D. Elvira,⁴⁵ Y. Enari,¹⁴ H. Evans,⁴⁹ A. Evdokimov,⁴⁶ V. N. Evdokimov,³⁴ A. Fauré,¹⁵ L. Feng,⁴⁷ T. Ferbel,⁶³ F. Fiedler,²¹ F. Filthaut,^{29,30} W. Fisher,⁵⁷ H. E. Fisk,⁴⁵ M. Fortner,⁴⁷ H. Fox,³⁹ J. Franc,⁷ S. Fuess,⁴⁵ P. H. Garbincius,⁴⁵ A. García-Bellido,⁶³ J. A. García-González,²⁸ V. Gavrilov,³² W. Geng,^{12,57} C. E. Gerber,⁴⁶ Y. Gershtein,⁶⁰ G. Ginther,⁴⁵ O. Gogota,³⁸ G. Golovanov,³¹ P. D. Grannis,⁶⁴ S. Greder,¹⁶ H. Greenlee,⁴⁵ G. Grenier,¹⁷ Ph. Gris,¹⁰ J.-F. Grivaz,¹³ A. Grohsjean,^{15,d} S. Grünendahl,⁴⁵ M. W. Grünewald,²⁶ T. Guillemain,¹³ G. Gutierrez,⁴⁵ P. Gutierrez,⁶⁷ J. Haley,⁶⁸ L. Han,⁴ K. Harder,⁴¹ A. Harel,⁶³ J. M. Hauptman,⁵² J. Hays,⁴⁰ T. Head,⁴¹ T. Hebbeker,¹⁸ D. Hedin,⁴⁷ H. Hegab,⁶⁸ A. P. Heinson,⁴³ U. Heintz,⁷⁰ C. Hensel,¹ I. Heredia-De La Cruz,^{28,d} K. Herner,⁴⁵ G. Hesketh,^{41,f} M. D. Hildreth,⁵¹ R. Hirosky,⁷⁴ T. Hoang,⁴⁴ J. D. Hobbs,⁶⁴ B. Hoeneisen,⁹ J. Hogan,⁷³ M. Hohlfeld,²¹ J. L. Holzbauer,⁵⁸ I. Howley,⁷¹ Z. Hubacek,^{7,15} V. Hynek,⁷ I. Iashvili,⁶² Y. Ilchenko,⁷² R. Illingworth,⁴⁵ A. S. Ito,⁴⁵ S. Jabeen,^{45,m} M. Jaffré,¹³ A. Jayasinghe,⁶⁷ M. S. Jeong,²⁷ R. Jesik,⁴⁰ P. Jiang,^{4,*} K. Johns,⁴² E. Johnson,⁵⁷ M. Johnson,⁴⁵ A. Jonckheere,⁴⁵ P. Jonsson,⁴⁰ J. Joshi,⁴³ A. W. Jung,^{45,o} A. Juste,³⁶ E. Kajfasz,¹² D. Karmanov,³³ I. Katsanos,⁵⁹ M. Kaur,²³ R. Kehoe,⁷² S. Kermiche,¹² N. Khalatyan,⁴⁵ A. Khanov,⁶⁸ A. Kharchilava,⁶² Y. N. Kharzheev,³¹ I. Kiselevich,³² J. M. Kohli,²³ A. V. Kozelov,³⁴ J. Kraus,⁵⁸ A. Kumar,⁶² A. Kupco,⁸ T. Kurča,¹⁷ V. A. Kuzmin,³³ S. Lammers,⁴⁹ P. Lebrun,¹⁷ H. S. Lee,²⁷ S. W. Lee,⁵² W. M. Lee,⁴⁵ X. Lei,⁴² J. Lellouch,¹⁴ D. Li,¹⁴ H. Li,⁷⁴ L. Li,⁴³ Q. Z. Li,⁴⁵ J. K. Lim,²⁷ D. Lincoln,⁴⁵ J. Linnemann,⁵⁷ V. V. Lipaev,^{34,*} R. Lipton,⁴⁵ H. Liu,⁷² Y. Liu,⁴ A. Lobodenko,³⁵ M. Lokajicek,⁸ R. Lopes de Sa,⁴⁵ R. Luna-Garcia,^{28,g} A. L. Lyon,⁴⁵ A. K. A. Maciel,¹ R. Madar,¹⁹ R. Magaña-Villalba,²⁸ S. Malik,⁵⁹ V. L. Malyshev,³¹ J. Mansour,²⁰ J. Martínez-Ortega,²⁸ R. McCarthy,⁶⁴ C. L. McGivern,⁴¹ M. M. Meijer,^{29,30} A. Melnitchouk,⁴⁵ D. Menezes,⁴⁷ P. G. Mercadante,³ M. Merkin,³³ A. Meyer,¹⁸ J. Meyer,^{20,i} F. Miconi,¹⁶ N. K. Mondal,²⁵ M. Mulhearn,⁷⁴ E. Nagy,¹² M. Narain,⁷⁰ R. Nayyar,⁴² H. A. Neal,⁵⁶ J. P. Negret,⁵ P. Neustroev,³⁵ H. T. Nguyen,⁷⁴ T. Nunnemann,²² J. Orduna,⁷⁰ N. Osman,¹² A. Pal,⁷¹ N. Parashar,⁵⁰ V. Parihar,⁷⁰ S. K. Park,²⁷ R. Partridge,^{70,e} N. Parua,⁴⁹ A. Patwa,^{65,j} B. Penning,⁴⁰ M. Perfilov,³³ Y. Peters,⁴¹ K. Petridis,⁴¹ G. Petrillo,⁶³ P. Pétroff,¹³ M.-A. Pleier,⁶⁵ V. M. Podstavkov,⁴⁵ A. V. Popov,³⁴ M. Prewitt,⁷³ D. Price,⁴¹ N. Prokopenko,³⁴ J. Qian,⁵⁶ A. Quadt,²⁰ B. Quinn,⁵⁸ P. N. Ratoff,³⁹ I. Razumov,³⁴ I. Ripp-Baudot,¹⁶ F. Rizatdinova,⁶⁸ M. Rominsky,⁴⁵ A. Ross,³⁹ C. Royon,⁸ P. Rubinov,⁴⁵ R. Ruchti,⁵¹ G. Sajot,¹¹ A. Sánchez-Hernández,²⁸ M. P. Sanders,²² A. S. Santos,^{1,h} G. Savage,⁴⁵ M. Savitskyi,³⁸ L. Sawyer,⁵⁴ T. Scanlon,⁴⁰ R. D. Schamberger,⁶⁴ Y. Scheglov,³⁵ H. Schellman,^{69,48} M. Schott,²¹ C. Schwanenberger,⁴¹ R. Schwienhorst,⁵⁷ J. Sekaric,⁵³ H. Severini,⁶⁷ E. Shabalina,²⁰ V. Shary,¹⁵ S. Shaw,⁴¹ A. A. Shchukin,³⁴ V. Simak,⁷ P. Skubic,⁶⁷ P. Slattery,⁶³ G. R. Snow,⁵⁹ J. Snow,⁶⁶ S. Snyder,⁶⁵ S. Söldner-Rembold,⁴⁴ L. Sonnenschein,¹⁸ K. Soustruznik,⁶ J. Stark,¹¹ N. Stefaniuk,³⁸ D. A. Stoyanova,³⁴ M. Strauss,⁶⁷ L. Suter,⁴¹ P. Svoisky,⁷⁴ M. Titov,¹⁵ V. V. Tokmenin,³¹ Y.-T. Tsai,⁶³ D. Tsybychev,⁶⁴ B. Tuchming,¹⁵ C. Tully,⁶¹ L. Uvarov,³⁵ S. Uvarov,³⁵ S. Uzunyan,⁴⁷ R. Van Kooten,⁴⁹ W. M. van Leeuwen,²⁹ N. Varelas,⁴⁶ E. W. Varnes,⁴² I. A. Vasilyev,³⁴ A. Y. Verkheev,³¹ L. S. Vertogradov,³¹ M. Verzocchi,⁴⁵ M. Vesterinen,⁴¹ D. Vilanova,¹⁵ P. Vokac,⁷ H. D. Wahl,⁴⁴ M. H. L. S. Wang,⁴⁵ J. Warchol,⁵¹ G. Watts,⁷⁵ M. Wayne,⁵¹ J. Weichert,²¹ L. Welty-Rieger,⁴⁸ M. R. J. Williams,^{49,n} G. W. Wilson,⁵³ M. Wobisch,⁵⁴ D. R. Wood,⁵⁵ T. R. Wyatt,⁴¹ Y. Xie,⁴⁵ R. Yamada,⁴⁵ S. Yang,⁴ T. Yasuda,⁴⁵ Y. A. Yatsunenko,³¹ W. Ye,⁶⁴ Z. Ye,⁴⁵ H. Yin,⁴⁵ K. Yip,⁶⁵ S. W. Youn,⁴⁵ J. M. Yu,⁵⁶ J. Zennamo,⁶² T. G. Zhao,⁴¹ B. Zhou,⁵⁶ J. Zhu,⁵⁶ M. Zielinski,⁶³ D. Zieminska,⁴⁹ and L. Zivkovic¹⁴

(D0 Collaboration)

¹LAFEX, Centro Brasileiro de Pesquisas Físicas, Rio de Janeiro, RJ 22290, Brazil

²Universidade do Estado do Rio de Janeiro, Rio de Janeiro, RJ 20550, Brazil

³Universidade Federal do ABC, Santo André, SP 09210, Brazil

⁴University of Science and Technology of China, Hefei 230026, People's Republic of China

- ⁵*Universidad de los Andes, Bogotá, 111711, Colombia*
- ⁶*Charles University, Faculty of Mathematics and Physics, Center for Particle Physics, 116 36 Prague 1, Czech Republic*
- ⁷*Czech Technical University in Prague, 116 36 Prague 6, Czech Republic*
- ⁸*Institute of Physics, Academy of Sciences of the Czech Republic, 182 21 Prague, Czech Republic*
- ⁹*Universidad San Francisco de Quito, Quito, Ecuador*
- ¹⁰*LPC, Université Blaise Pascal, CNRS/IN2P3, Clermont, F-63178 Aubière Cedex, France*
- ¹¹*LPSC, Université Joseph Fourier Grenoble 1, CNRS/IN2P3, Institut National Polytechnique de Grenoble, F-38026 Grenoble Cedex, France*
- ¹²*CPPM, Aix-Marseille Université, CNRS/IN2P3, F-13288 Marseille Cedex 09, France*
- ¹³*LAL, Univ. Paris-Sud, CNRS/IN2P3, Université Paris-Saclay, F-91898 Orsay Cedex, France*
- ¹⁴*LPNHE, Universités Paris VI and VII, CNRS/IN2P3, F-75005 Paris, France*
- ¹⁵*CEA Saclay, Irfu, SPP, F-91191 Gif-Sur-Yvette Cedex, France*
- ¹⁶*IPHC, Université de Strasbourg, CNRS/IN2P3, F-67037 Strasbourg, France*
- ¹⁷*IPNL, Université Lyon 1, CNRS/IN2P3, F-69622 Villeurbanne Cedex, France and Université de Lyon, F-69361 Lyon CEDEX 07, France*
- ¹⁸*III. Physikalisches Institut A, RWTH Aachen University, 52056 Aachen, Germany*
- ¹⁹*Physikalisches Institut, Universität Freiburg, 79085 Freiburg, Germany*
- ²⁰*II. Physikalisches Institut, Georg-August-Universität Göttingen, 37073 Göttingen, Germany*
- ²¹*Institut für Physik, Universität Mainz, 55099 Mainz, Germany*
- ²²*Ludwig-Maximilians-Universität München, 80539 München, Germany*
- ²³*Panjab University, Chandigarh 160014, India*
- ²⁴*Delhi University, Delhi-110 007, India*
- ²⁵*Tata Institute of Fundamental Research, Mumbai-400 005, India*
- ²⁶*University College Dublin, Dublin 4, Ireland*
- ²⁷*Korea Detector Laboratory, Korea University, Seoul, 02841, Korea*
- ²⁸*CINVESTAV, Mexico City 07360, Mexico*
- ²⁹*Nikhef, Science Park, 1098 XG Amsterdam, Netherlands*
- ³⁰*Radboud University Nijmegen, 6525 AJ Nijmegen, Netherlands*
- ³¹*Joint Institute for Nuclear Research, Dubna 141980, Russia*
- ³²*Institute for Theoretical and Experimental Physics, Moscow 117259, Russia*
- ³³*Moscow State University, Moscow 119991, Russia*
- ³⁴*Institute for High Energy Physics, Protvino, Moscow region 142281, Russia*
- ³⁵*Petersburg Nuclear Physics Institute, St. Petersburg 188300, Russia*
- ³⁶*Institució Catalana de Recerca i Estudis Avançats (ICREA) and Institut de Física d'Altes Energies (IFAE), 08193 Bellaterra (Barcelona), Spain*
- ³⁷*Uppsala University, 751 05 Uppsala, Sweden*
- ³⁸*Taras Shevchenko National University of Kyiv, Kiev, 01601, Ukraine*
- ³⁹*Lancaster University, Lancaster LA1 4YB, United Kingdom*
- ⁴⁰*Imperial College London, London SW7 2AZ, United Kingdom*
- ⁴¹*The University of Manchester, Manchester M13 9PL, United Kingdom*
- ⁴²*University of Arizona, Tucson, Arizona 85721, USA*
- ⁴³*University of California Riverside, Riverside, California 92521, USA*
- ⁴⁴*Florida State University, Tallahassee, Florida 32306, USA*
- ⁴⁵*Fermi National Accelerator Laboratory, Batavia, Illinois 60510, USA*
- ⁴⁶*University of Illinois at Chicago, Chicago, Illinois 60607, USA*
- ⁴⁷*Northern Illinois University, DeKalb, Illinois 60115, USA*
- ⁴⁸*Northwestern University, Evanston, Illinois 60208, USA*
- ⁴⁹*Indiana University, Bloomington, Indiana 47405, USA*
- ⁵⁰*Purdue University Calumet, Hammond, Indiana 46323, USA*
- ⁵¹*University of Notre Dame, Notre Dame, Indiana 46556, USA*
- ⁵²*Iowa State University, Ames, Iowa 50011, USA*
- ⁵³*University of Kansas, Lawrence, Kansas 66045, USA*
- ⁵⁴*Louisiana Tech University, Ruston, Louisiana 71272, USA*
- ⁵⁵*Northeastern University, Boston, Massachusetts 02115, USA*
- ⁵⁶*University of Michigan, Ann Arbor, Michigan 48109, USA*
- ⁵⁷*Michigan State University, East Lansing, Michigan 48824, USA*
- ⁵⁸*University of Mississippi, University, Mississippi 38677, USA*
- ⁵⁹*University of Nebraska, Lincoln, Nebraska 68588, USA*
- ⁶⁰*Rutgers University, Piscataway, New Jersey 08855, USA*

⁶¹*Princeton University, Princeton, New Jersey 08544, USA*⁶²*State University of New York, Buffalo, New York 14260, USA*⁶³*University of Rochester, Rochester, New York 14627, USA*⁶⁴*State University of New York, Stony Brook, New York 11794, USA*⁶⁵*Brookhaven National Laboratory, Upton, New York 11973, USA*⁶⁶*Langston University, Langston, Oklahoma 73050, USA*⁶⁷*University of Oklahoma, Norman, Oklahoma 73019, USA*⁶⁸*Oklahoma State University, Stillwater, Oklahoma 74078, USA*⁶⁹*Oregon State University, Corvallis, Oregon 97331, USA*⁷⁰*Brown University, Providence, Rhode Island 02912, USA*⁷¹*University of Texas, Arlington, Texas 76019, USA*⁷²*Southern Methodist University, Dallas, Texas 75275, USA*⁷³*Rice University, Houston, Texas 77005, USA*⁷⁴*University of Virginia, Charlottesville, Virginia 22904, USA*⁷⁵*University of Washington, Seattle, Washington 98195, USA*

(Received 12 May 2016; published 1 June 2016)

We measure the forward-backward asymmetries A_{FB} of charged Ξ and Ω baryons produced in $p\bar{p}$ collisions recorded by the D0 detector at the Fermilab Tevatron collider at $\sqrt{s} = 1.96$ TeV as a function of the baryon rapidity y . We find that the asymmetries A_{FB} for charged Ξ and Ω baryons are consistent with zero within statistical uncertainties.

DOI: 10.1103/PhysRevD.93.112001

I. INTRODUCTION

We present a study of the forward-backward asymmetries A_{FB} for the production of charged Ξ and Ω baryons in $p\bar{p}$ collisions at a center-of-mass energy $\sqrt{s} = 1.96$ TeV, recorded by the D0 detector at the Fermilab Tevatron collider.

We previously performed a study of A_{FB} for Λ and $\bar{\Lambda}$ production [1], where A_{FB} is defined as the relative excess of Λ ($\bar{\Lambda}$) baryons produced with longitudinal momentum p_z in the p (\bar{p}) direction. These results are in agreement with the observations in a wide range of proton collision experiments that the $\bar{\Lambda}/\Lambda$ production ratio follows a universal function of the “rapidity loss” $y_p - y$ between the beam proton and the produced $\bar{\Lambda}$ or Λ baryon which does not depend significantly on \sqrt{s} or on the nature of the target p , \bar{p} , Be, or Pb (see Ref. [1] and references therein). These results support the view that a strange quark produced directly in the hard scattering of pointlike partons, or indirectly in the subsequent showering, can coalesce with a diquark remnant of the beam particle to produce a Λ baryon with a probability that increases as the rapidity difference between the incoming proton and outgoing Λ baryon decreases.

If this hypothesis is correct, we also expect $A_{\text{FB}} > 0$ for Λ_c ($\bar{\Lambda}_c$), and Λ_b ($\bar{\Lambda}_b$) production in which a c or b quark can coalesce with a diquark from the proton. For the B mesons and Ξ and Ω baryons, we expect $A_{\text{FB}} \approx 0$ since these particles do not share a diquark with the proton. Previous D0 measurements include $A_{\text{FB}}(B^-, B^+)$ [2] and $A_{\text{FB}}(\Lambda_b, \bar{\Lambda}_b)$ [3].

In this article, we present measurements of the forward-backward asymmetries of Ξ^\mp and Ω^\mp production, where we use the notation $\Xi^+ \equiv \Xi^-$ and $\Omega^+ \equiv \Omega^-$. The Ξ^- and Ξ^+ baryons are defined as “forward” if their p_z points in the p or \bar{p} direction, respectively. The asymmetry A_{FB} is defined as

*Deceased.

^aVisitor from Augustana College, Sioux Falls, SD 57197, USA.^bVisitor from Kiev Institute for Nuclear Research (KINR), Kyiv 03680, Ukraine.^cVisitor from The University of Liverpool, Liverpool L69 3BX, UK.^dVisitor from American Association for the Advancement of Science, Washington, DC 20005, USA.^eVisitor from Deutsches Elektronen-Synchrotron (DESY), Notkestrasse 85, Germany.^fVisitor from CONACyT, M-03940 Mexico City, Mexico.^gVisitor from University College London, London WC1E 6BT, UK.^hVisitor from University of Maryland, College Park, MD 20742, USA.ⁱVisitor from Purdue University, West Lafayette, IN 47907, USA.^jVisitor from Centro de Investigacion en Computacion—IPN, CP 07738 Mexico City, Mexico.^kVisitor from Karlsruhe Institut für Technologie (KIT)—Steinbuch Centre for Computing (SCC), D-76128 Karlsruhe, Germany.^lVisitor from SLAC, Menlo Park, CA 94025, USA.^mVisitor from Office of Science, U.S. Department of Energy, Washington, D.C. 20585, USA.ⁿVisitor from Universidade Estadual Paulista, São Paulo, SP 01140, Brazil.^oVisitor from European Organization for Nuclear Research (CERN), CH-1211 Geneva, Switzerland.

$$A_{\text{FB}} \equiv \frac{\sigma_{\text{F}}(\Xi^-) - \sigma_{\text{B}}(\Xi^-) + \sigma_{\text{F}}(\Xi^+) - \sigma_{\text{B}}(\Xi^+)}{\sigma_{\text{F}}(\Xi^-) + \sigma_{\text{B}}(\Xi^-) + \sigma_{\text{F}}(\Xi^+) + \sigma_{\text{B}}(\Xi^+)}, \quad (1)$$

where σ_{F} and σ_{B} are the forward and backward cross sections of Ξ^- or Ξ^+ production, and similarly for Ω^\mp baryons. The measurements include Ξ^\mp and Ω^\mp baryons that are either directly produced or decay products of heavier hadrons. The measurement strategy for the asymmetry A_{FB} of Ξ^\mp and Ω^\mp baryons presented here closely follows the analysis method used to determine A_{FB} for Λ and $\bar{\Lambda}$ baryons in Ref. [1].

II. DETECTOR AND DATA

The D0 detector is described in detail in Refs. [4–7]. The collision region is surrounded by a central tracking system that comprises a silicon microstrip vertex detector and a central fiber tracker, both located within a 1.9 T superconducting solenoidal magnet [4], surrounded successively by the liquid-argon/uranium calorimeters, a layer of the muon system [5], comprising drift chambers and scintillation trigger counters, the 1.8 T magnetized iron toroids, and two additional muon detector layers after the toroids.

The longitudinal momentum p_z and the rapidity $y \equiv \ln[(E + p_z)/(E - p_z)]/2$ are both measured with respect to the proton beam direction in the $p\bar{p}$ center-of-mass frame where E is the energy of the baryon. We present results for the full integrated luminosity of 10.4 fb^{-1} , collected from 2002 to 2011, using two data sets (i) $p\bar{p} \rightarrow \Xi^\mp X$, and (ii) $p\bar{p} \rightarrow \mu\Xi^\mp X$. The first data set is unbiased since it is collected using a prescaled trigger on beam crossing (“zero bias events”) or with a prescaled trigger on energy deposited in the forward counters (“minimum bias events”). The second data set is selected with a suite of single muon triggers which implies that most events contain heavy-quark (b or c) decays. This data set is defined using the same muon triggers and muon selections as in Refs. [8,9]. The muon data provides a sizable data set that adds additional statistics for the analysis. For Ω^\pm there are fewer events, so we only present results for the set $p\bar{p} \rightarrow \mu\Omega^\mp X$.

We observe Ξ baryons through their decays $\Xi^- \rightarrow \Lambda\pi^-$ and $\Xi^+ \rightarrow \bar{\Lambda}\pi^+$, and Ω baryons through their decays $\Omega^- \rightarrow \Lambda K^-$ and $\Omega^+ \rightarrow \bar{\Lambda}K^+$, with $\Lambda \rightarrow p\pi^-$ and $\bar{\Lambda} \rightarrow \bar{p}\pi^+$ in both cases. The Λ and $\bar{\Lambda}$ candidates are reconstructed from pairs of oppositely curved tracks with a common vertex (V^0). Each track is required to have a nonzero impact parameter in the transverse plane (IP) with respect to the $p\bar{p}$ interaction vertex with a significance of at least two standard deviations. The proton (pion) mass is assigned to the daughter track with larger (smaller) total momentum since the decay $\Lambda \rightarrow p\pi$ is just above threshold. The invariant mass of the (p, π^-) or (\bar{p}, π^+) pair is required to be in the interval $1.105 < M(p\pi) < 1.125 \text{ GeV}$ [1]. We require Λ and $\bar{\Lambda}$ candidates with $1.5 < p_T < 25 \text{ GeV}$ and

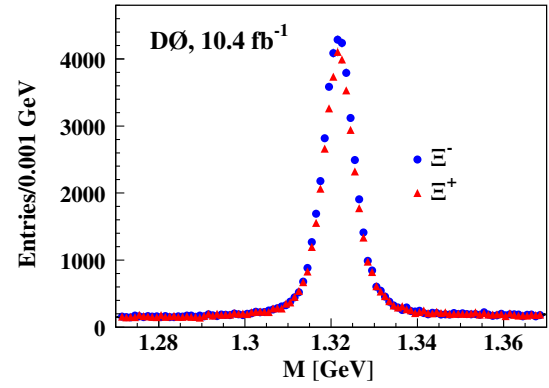


FIG. 1. Invariant mass distributions of reconstructed $\Xi^- \rightarrow \Lambda\pi^-$ (circles) and $\Xi^+ \rightarrow \bar{\Lambda}\pi^+$ (triangles) for $p\bar{p} \rightarrow \mu\Xi^\mp X$ data.

pseudorapidity $|\eta| < 2.2$ [10], and their IP must be nonzero with a significance greater than two standard deviations.

The Λ ($\bar{\Lambda}$) candidate is combined with a negatively (positively) charged-particle track with separation in the transverse plane from the primary vertex with significance greater than three standard deviations and a good vertex with the Λ ($\bar{\Lambda}$) candidate. This track is assigned the pion mass for Ξ 's or the kaon mass for Ω 's. The Ξ^\mp or Ω^\mp candidates are required to have an IP consistent with zero within three standard deviations. The observed decay lengths in the transverse plane of the Λ and Ξ^- or Ω^- (or $\bar{\Lambda}$ and Ξ^+ or Ω^+) are required to be greater than 4 mm. The invariant mass for the Ξ^\mp candidate is required to be in the interval $1.2 < M(\Lambda\pi) < 1.5 \text{ GeV}$ and $1.55 < M(\bar{\Lambda}K) < 1.85 \text{ GeV}$ for Ω^\mp candidates. The kinematic selections for the Ξ^\mp and Ω^\mp candidates are $p_T > 2.0 \text{ GeV}$ and $|\eta| < 2.2$. The pion or kaon track and the two daughter tracks of the Λ baryon are required to be different from any track associated with a muon. The invariant mass distributions for the decays $\Xi^- \rightarrow \Lambda\pi^-$ and $\Xi^+ \rightarrow \bar{\Lambda}\pi^+$ are shown in Fig. 1 and for the decays $\Omega^- \rightarrow \Lambda K^-$ and $\Omega^+ \rightarrow \bar{\Lambda}K^+$ in Fig. 2.

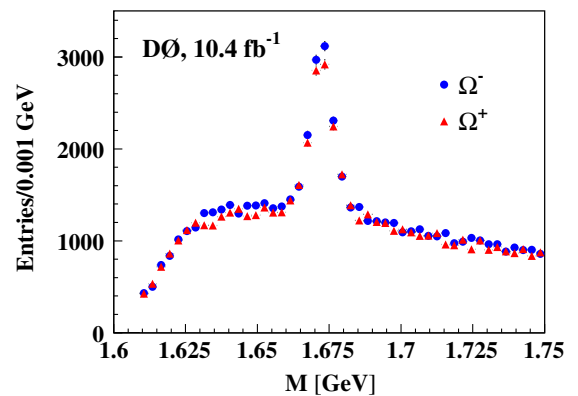


FIG. 2. Invariant mass distributions of reconstructed $\Omega^- \rightarrow \Lambda K^-$ (circles) and $\Omega^+ \rightarrow \bar{\Lambda}K^+$ (triangles) for $p\bar{p} \rightarrow \mu\Omega^\mp X$ data.

III. RAW ASYMMETRIES AND DETECTOR EFFECTS

We obtain the numbers $N_F(\Xi^\mp)$ and $N_B(\Xi^\mp)$ of reconstructed Ξ^\mp baryons in the forward and backward categories in each bin of $|y|$ by counting Ξ^\mp candidates in the signal region, $1.305 < M(\Lambda\pi) < 1.335$ GeV, and subtracting the counts in two sideband regions, defined by $1.2775 < M(\Lambda\pi) < 1.2925$ GeV and $1.3475 < M(\Lambda\pi) < 1.3625$ GeV. The signal region for Ω^\mp candidates is $1.6575 < M(\Lambda K) < 1.6875$ GeV, and the sideband regions are $1.630 < M(\Lambda K) < 1.645$ GeV and $1.700 < M(\Lambda K) < 1.715$ GeV.

The normalization factor N and the three raw asymmetries A'_{FB} , A'_{NS} , and A'_{Ξ} are defined by

$$\begin{aligned} N_F(\Xi^-) &\equiv N(1 + A'_{FB})(1 - A'_{NS})(1 + A'_{\Xi}), \\ N_B(\Xi^-) &\equiv N(1 - A'_{FB})(1 + A'_{NS})(1 + A'_{\Xi}), \\ N_F(\Xi^+) &\equiv N(1 + A'_{FB})(1 + A'_{NS})(1 - A'_{\Xi}), \\ N_B(\Xi^+) &\equiv N(1 - A'_{FB})(1 - A'_{NS})(1 - A'_{\Xi}), \end{aligned} \quad (2)$$

and similarly for Ω . The raw asymmetries A'_{FB} , A'_{NS} , and A'_{Ξ} have contributions from the physical asymmetries A_{FB} , A_{NS} , and A_{Ξ} , and from detector effects. The

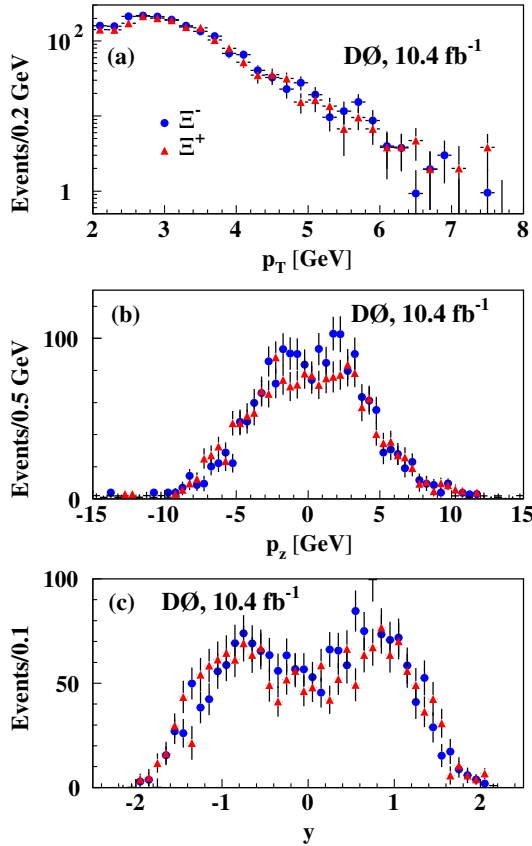


FIG. 3. Distributions of p_T , p_z , and y of reconstructed Ξ^- (circles) and Ξ^+ candidates (triangles) with $p_T > 2$ GeV, for the minimum bias data sample $p\bar{p} \rightarrow \Xi^\mp X$.

forward-backward asymmetry A_{FB} measures the relative excess of Ξ^- (Ξ^+) baryons with p_z in the p (\bar{p}) direction. The asymmetry A_{NS} is given by the relative excess of the sum of Ξ^- and Ξ^+ baryons with p_z in the \bar{p} beam direction (north) with respect to the p beam direction (south). The asymmetry A_{Ξ} is the relative excess of negatively charged over positively charged baryons.

The initial $p\bar{p}$ state is invariant with respect to CP conjugation, which changes the sign of A_{NS} and A_{Ξ} , while A_{FB} remains unchanged. A nonzero value of A_{NS} or A_{Ξ} would indicate CP violation.

The asymmetry A'_{NS} is mainly due to differences in the product of the acceptance and efficiency between the northern hemisphere of the $D\phi$ detector with respect to the southern hemisphere. The difference in reconstruction efficiencies of Ξ^- and Ξ^+ baryons caused by the different inelastic interaction cross sections of p and \bar{p} with the detector material creates the additional asymmetry A'_{Ξ} [1].

The raw asymmetries including terms up to second order in the asymmetries are given by

$$A'_{FB} = A'_{NS}A'_{\Xi} + \frac{N_F(\Xi^-) - N_B(\Xi^-) + N_F(\Xi^+) - N_B(\Xi^+)}{N_F(\Xi^-) + N_B(\Xi^-) + N_F(\Xi^+) + N_B(\Xi^+)}, \quad (3)$$

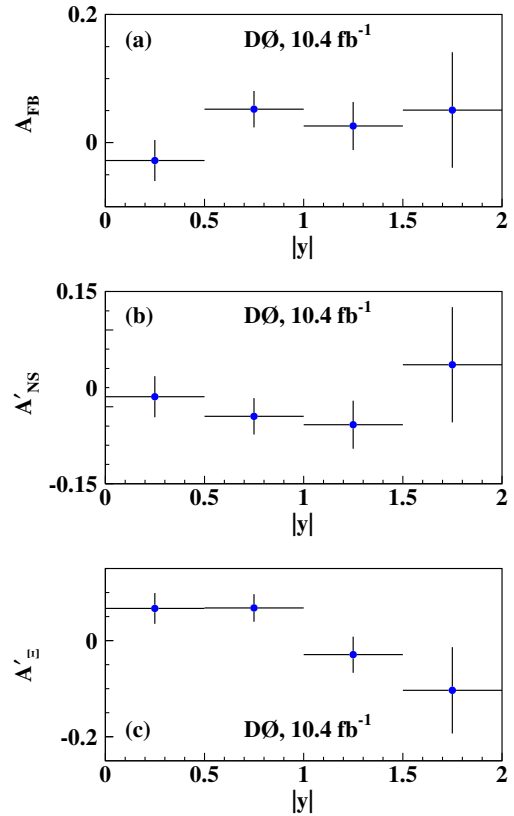


FIG. 4. Asymmetries $A'_{FB} = A_{FB}$, A'_{NS} , and A'_{Ξ} of reconstructed Ξ^- and Ξ^+ candidates with $p_T > 2$ GeV, as a function of $|y|$, for the minimum bias data sample $p\bar{p} \rightarrow \Xi^\mp X$. The uncertainties are statistical.

TABLE I. Forward-backward asymmetry A_{FB} of Ξ^\mp baryons with $p_T > 2$ GeV in minimum bias events, $p\bar{p} \rightarrow \Xi^\mp X$, and muon events $p\bar{p} \rightarrow \mu\Xi^\mp X$, and A_{FB} of Ω^- and Ω^+ baryons with $p_T > 2$ GeV in muon events $p\bar{p} \rightarrow \mu\Omega^\mp X$. The first uncertainty is statistical, the second is systematic due to the detector asymmetry $A'_{\text{NS}}A'_{\Xi}$.

$ y $	$A_{\text{FB}} \times 100$ (Ξ^\mp , min. bias)	$A_{\text{FB}} \times 100$ (Ξ^\mp , with μ)	$A_{\text{FB}} \times 100$ (Ω^\mp , with μ)
0.0 to 0.5	$-2.78 \pm 3.20 \pm 0.34$	$-0.20 \pm 0.72 \pm 0.01$	$-3.43 \pm 2.90 \pm 0.13$
0.5 to 1.0	$5.23 \pm 2.85 \pm 0.55$	$-0.13 \pm 0.66 \pm 0.03$	$3.25 \pm 2.78 \pm 0.10$
1.0 to 1.5	$2.61 \pm 3.75 \pm 0.45$	$1.55 \pm 0.77 \pm 0.05$	$0.46 \pm 3.52 \pm 0.14$
1.5 to 2.0	$5.09 \pm 9.00 \pm 1.64$	$-1.14 \pm 2.05 \pm 0.27$	$5.75 \pm 10.86 \pm 5.70$

$$A'_{\text{NS}} = A'_{\text{FB}}A'_{\Xi} + \frac{-N_{\text{F}}(\Xi^-) + N_{\text{B}}(\Xi^-) + N_{\text{F}}(\Xi^+) - N_{\text{B}}(\Xi^+)}{N_{\text{F}}(\Xi^-) + N_{\text{B}}(\Xi^-) + N_{\text{F}}(\Xi^+) + N_{\text{B}}(\Xi^+)}, \quad (4)$$

$$A'_{\Xi} = A'_{\text{FB}}A'_{\text{NS}} + \frac{N_{\text{F}}(\Xi^-) + N_{\text{B}}(\Xi^-) - N_{\text{F}}(\Xi^+) - N_{\text{B}}(\Xi^+)}{N_{\text{F}}(\Xi^-) + N_{\text{B}}(\Xi^-) + N_{\text{F}}(\Xi^+) + N_{\text{B}}(\Xi^+)}. \quad (5)$$

The polarities of the solenoid and toroid magnets were reversed about once every two weeks during data taking to collect approximately the same number of events for each of the four solenoid-toroid polarity combinations. We apply weights to equalize the sums of Ξ^- and Ξ^+ candidates reconstructed for each of the four polarity combinations. This averaging over magnet polarities cancels contributions from the detector geometry to A'_{FB} and A'_{Ξ} , but not to A'_{NS} [1].

The raw asymmetry A'_{FB} has negligible contributions from detector effects after averaging over solenoid and toroid magnet polarities. The raw asymmetries A'_{NS} and A'_{Ξ} are dominated by detector effects [1]. The quadratic term

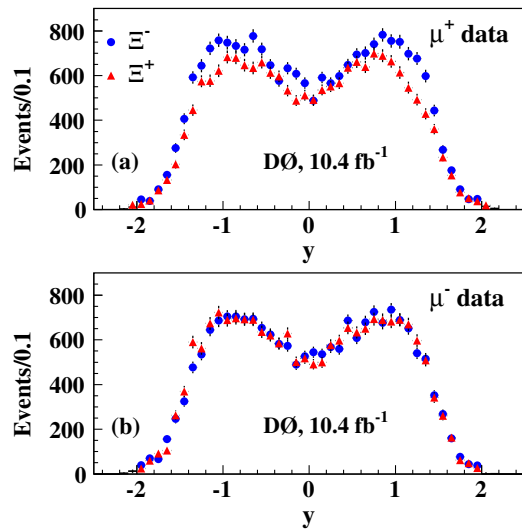


FIG. 5. Distributions of rapidity y for reconstructed Ξ^- (circles) and Ξ^+ candidates (triangles) in events with a (a) positively or (b) negatively charged muon for Ξ^\mp candidates with $p_T > 2$ GeV.

$A'_{\text{NS}}A'_{\Xi}$ in Eq. (3) corrects A'_{FB} for the detector effects A'_{NS} and A'_{Ξ} on the particle counts $N_{\text{F}}(\Xi^\mp)$ and $N_{\text{B}}(\Xi^\mp)$. We can therefore set $A'_{\text{FB}} = A_{\text{FB}}$ where A_{FB} is defined in Eq. (1).

IV. MINIMUM BIAS SAMPLE EVENTS $p\bar{p} \rightarrow \Xi^\mp X$

The minimum bias sample contains 3.7×10^3 reconstructed Ξ^\mp candidates with $p_T > 2$ GeV. Distributions of p_T , p_z , and y for the Ξ^\mp candidates are shown in Fig. 3 and the corresponding raw asymmetries

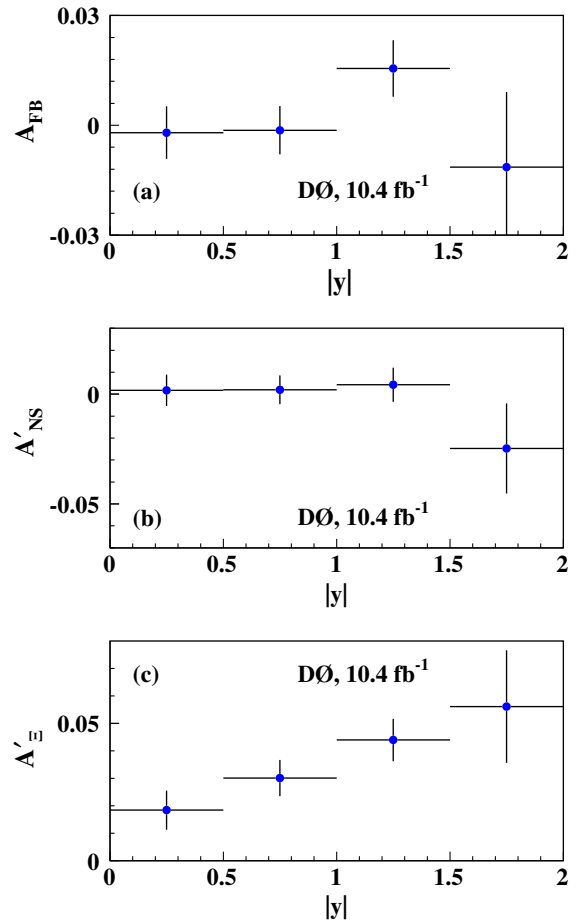


FIG. 6. Asymmetries $A'_{\text{FB}} = A_{\text{FB}}$, A'_{NS} , and A'_{Ξ} of reconstructed Ξ^- and Ξ^+ candidates with $p_T > 2$ GeV, as a function of $|y|$, for $p\bar{p} \rightarrow \mu\Xi^\mp X$ events. The uncertainties are statistical.

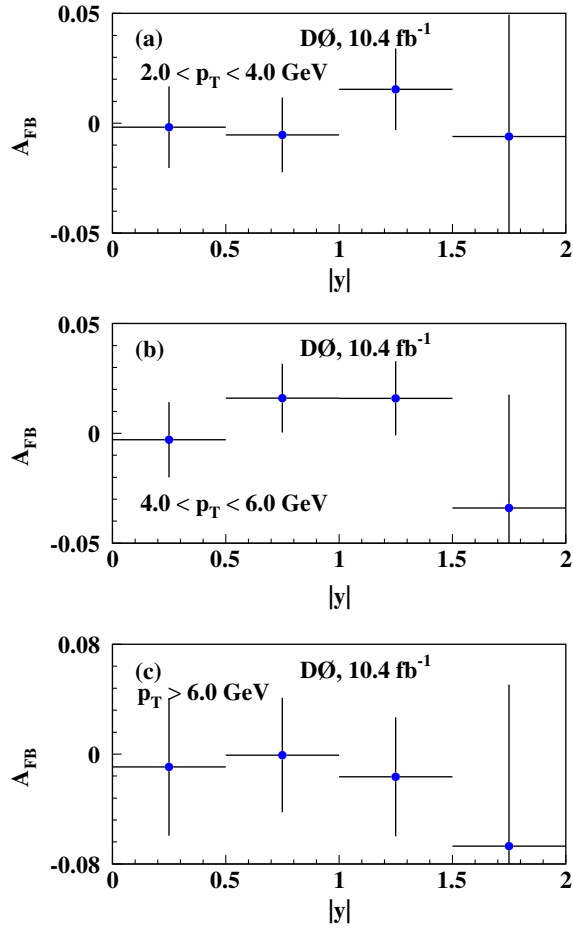


FIG. 7. Asymmetry $A'_{\text{FB}} = A_{\text{FB}}$ as a function of $|y|$ for $p\bar{p} \rightarrow \mu\Xi^{\mp}X$ events with (a) $2.0 < p_T < 4.0$ GeV, (b) $4.0 < p_T < 6.0$ GeV, and (c) $p_T > 6.0$ GeV. The uncertainties are statistical.

$A'_{\text{FB}} = A_{\text{FB}}$, A'_{NS} , and A'_{Ξ} in Fig. 4. These asymmetries are calculated using Eqs. (3)–(5), neglecting the quadratic terms since they are small compared to the statistical uncertainties. The correction $A'_{\text{NS}}A'_{\Xi}$ needed to obtain $A'_{\text{FB}} = A_{\text{FB}}$ is measured to be consistent with zero within statistical uncertainties; see Figs. 4(b) and 4(c). Thus, we choose not to apply this correction, but rather we take the full measured detector asymmetry $A'_{\text{NS}}A'_{\Xi}$ as the systematic uncertainty on the measurement of A_{FB} . The results are summarized in Table I.

V. MUON SAMPLE EVENTS $p\bar{p} \rightarrow \mu\Xi^{\mp}X$ AND $p\bar{p} \rightarrow \mu\Omega^{\mp}X$

To study the asymmetries using a larger data set, we consider $p\bar{p} \rightarrow \mu\Xi^{\mp}X$ and $p\bar{p} \rightarrow \mu\Omega^{\mp}X$ events taken from the single muon trigger sample. Charged particles with transverse momentum in the range $1.5 < p_T < 25$ GeV and $|\eta| < 2.2$ are considered as muon candidates. Muon candidates are further selected by matching central tracks with a segment reconstructed in the muon system and by

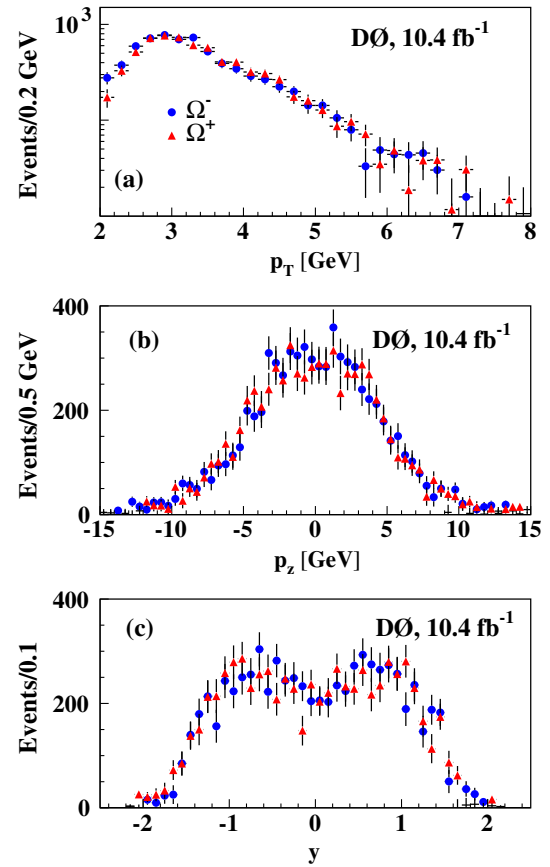


FIG. 8. Distributions of p_T , p_z , and y of reconstructed Ω^- (circles) and Ω^+ (triangles) with $p_T > 2$ GeV, for the data sample $p\bar{p} \rightarrow \mu\Omega^{\mp}X$.

applying tight quality requirements aimed at reducing false matching and background from cosmic rays and beam halo. To ensure that the muon candidate traverses the detector, including all three layers of the muon system, we require either $p_T > 4.2$ GeV or $|p_z| > 5.4$ GeV [8,9]. The inclusive muon sample contains 2.2×10^9 reconstructed muons and 7.7×10^4 reconstructed Ξ^- and Ξ^+ candidates with

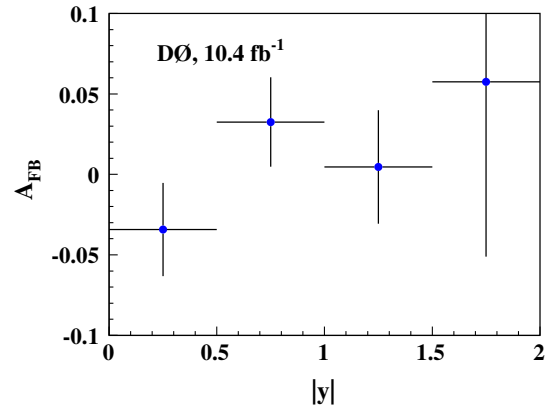


FIG. 9. Asymmetry A_{FB} as a function of $|y|$ for events $p\bar{p} \rightarrow \mu\Omega^{\mp}X$ for $p_T > 2$ GeV. The uncertainties are statistical.

$p_T > 2$ GeV, as well as 1.4×10^4 reconstructed Ω^- and Ω^+ candidates.

Rapidity distributions for reconstructed Ξ^- and Ξ^+ candidates are shown in Fig. 5. From these distributions we observe that (i) the detection efficiency for Ξ^- baryons is larger than for Ξ^+ baryons as explained above, and (ii) there are more $\Xi^\mp \mu^\pm$ than $\Xi^\mp \mu^\mp$ events. An example of a process with a correlated $\Xi^- \mu^+$ pair is the decay $\Xi_c^0 \rightarrow \Xi^- \mu^+ X$. We find that the asymmetry A'_{FB} obtained with events containing a μ^+ is consistent with the corresponding asymmetry with μ^- within statistical uncertainties. We therefore combine the μ^+ and μ^- samples to obtain the asymmetries presented in Figs. 6 and 7.

The p_T , p_z , and y distributions for $p\bar{p} \rightarrow \mu\Omega^\mp X$ events are shown in Fig. 8, and the corresponding asymmetry A_{FB} is presented in Fig. 9. The Ξ^\mp and Ω^\mp asymmetries are summarized in Table I.

VI. CONCLUSIONS

We have measured the forward-backward asymmetries A_{FB} in $p\bar{p} \rightarrow \Xi^\mp X$, $p\bar{p} \rightarrow \mu\Xi^\mp X$, and $p\bar{p} \rightarrow \mu\Omega^\mp X$ events using 10.4 fb^{-1} of integrated luminosity recorded with the D0 detector. We find that A_{FB} for Ξ^\mp and Ω^\mp are consistent with zero within uncertainties.

ACKNOWLEDGMENTS

We thank the staffs at Fermilab and collaborating institutions, and acknowledge support from the

Department of Energy and National Science Foundation (United States of America); Alternative Energies and Atomic Energy Commission and National Center for Scientific Research/National Institute of Nuclear and Particle Physics (France); Ministry of Education and Science of the Russian Federation, National Research Center ‘‘Kurchatov Institute’’ of the Russian Federation, and Russian Foundation for Basic Research (Russia); National Council for the Development of Science and Technology and Carlos Chagas Filho Foundation for the Support of Research in the State of Rio de Janeiro (Brazil); Department of Atomic Energy and Department of Science and Technology (India); Administrative Department of Science, Technology and Innovation (Colombia); National Council of Science and Technology (Mexico); National Research Foundation of Korea (Korea); Foundation for Fundamental Research on Matter (The Netherlands); Science and Technology Facilities Council and The Royal Society (United Kingdom); Ministry of Education, Youth and Sports (Czech Republic); Bundesministerium für Bildung und Forschung (Federal Ministry of Education and Research) and Deutsche Forschungsgemeinschaft (German Research Foundation) (Germany); Science Foundation Ireland (Ireland); Swedish Research Council (Sweden); Chinese Academy of Sciences and National Natural Science Foundation of China (China); and Ministry of Education and Science of Ukraine (Ukraine).

-
- [1] V. M. Abazov *et al.* (D0 Collaboration), Measurement of the forward-backward asymmetry of Λ and $\bar{\Lambda}$ production in $p\bar{p}$ collisions, *Phys. Rev. D* **93**, 032002 (2016).
- [2] V. M. Abazov *et al.* (D0 Collaboration), Measurement of the Forward-Backward Asymmetry in the Production of B^\pm in $p\bar{p}$ Collisions at $\sqrt{s} = 1.96$ TeV, *Phys. Rev. Lett.* **114**, 051803 (2015).
- [3] V. M. Abazov *et al.* (D0 Collaboration), Measurement of the forward-backward asymmetry in Λ_b^0 and $\bar{\Lambda}_b^0$ baryon production in $p\bar{p}$ collisions at $\sqrt{s} = 1.96$ TeV, *Phys. Rev. D* **91**, 072008 (2015).
- [4] V. M. Abazov *et al.* (D0 Collaboration), The upgraded D0 detector, *Nucl. Instrum. Methods Phys. Res., Sect. A* **565**, 463 (2006).
- [5] V. M. Abazov *et al.* (D0 Collaboration), The muon system of the Run II D0 detector, *Nucl. Instrum. Methods Phys. Res., Sect. A* **552**, 372 (2005).
- [6] S. N. Ahmed *et al.*, The D0 silicon microstrip tracker, *Nucl. Instrum. Methods Phys. Res., Sect. A* **634**, 8 (2011).
- [7] R. Angstadt *et al.*, The layer 0 inner silicon detector of the D0 experiment, *Nucl. Instrum. Methods Phys. Res., Sect. A* **622**, 298 (2010).
- [8] V. M. Abazov *et al.* (D0 Collaboration), Measurement of the anomalous like-sign dimuon charge asymmetry with 9 fb^{-1} of $p\bar{p}$ collisions, *Phys. Rev. D* **84**, 052007 (2011).
- [9] V. M. Abazov *et al.* (D0 Collaboration), Study of CP -violating charge asymmetries of single muons and like-sign dimuons in $p\bar{p}$ collisions, *Phys. Rev. D* **89**, 012002 (2014).
- [10] The pseudorapidity is given by $\eta = -\ln[\tan(\theta/2)]$, where θ is the polar angle with respect to the proton beam direction